N O T I C E

THIS DOCUMENT HAS BEEN REPRODUCED FROM MICROFICHE. ALTHOUGH IT IS RECOGNIZED THAT CERTAIN PORTIONS ARE ILLEGIBLE, IT IS BEING RELEASED IN THE INTEREST OF MAKING AVAILABLE AS MUCH INFORMATION AS POSSIBLE

DOE/NASA/51044-16
NASA TM-81713

Response of Nickel Zinc Cells to Electric Vehicle Chopper Discharge Waveforms

Robert L. Cataldo
National Aeronautics and Space Administration
Lewis Research Center
Cleveland, Ohio 44135

Work performed for
U.S. DEPARTMENT OF ENERGY
Conservation and Solar Energy
Office of Transportation Programs
Washington, D.C. 20545
Under Interagency Agreement DE-AI01-77CS51044

Prepared for
Electric Vehicle Council Symposium VI
sponsored by the Electric Vehicle Council
Baltimore, Maryland, October 21-23, 1981

DOE/NASA/51044-16
NASA TM-81713

Response of Nickel Zinc Cells to Electric Vehicle Chopper Discharge Waveforms

Robert L. Cataldo
National Aeronautics and Space Administration
Lewis Research Center
Cleveland, Ohio 44135

Work performed for
U.S. DEPARTMENT OF ENERGY
Conservation and Solar Energy
Office of Transportation Programs
Washington, D.C. 20545
Under Interagency Agreement DE-AI01-77CS51044

Prepared for
Electric Vehicle Council Symposium VI
sponsored by the Electric Vehicle Council
Baltimore, Maryland, October 21-23, 1981

RESPONSE OF NICKEL TO ZINC CELLS TO ELECTRIC VEHICLE CHOPPER DISCHARGE WAVEFORMS

by Robert L. Cataldo

National Aeronautics and Space Administration
Lewis Research Center
Cleveland, Ohio 44135

ABSTRACT

The preliminary results of simulated electric vehicle chopper controlled discharge of a nickel/zinc (NiZn) battery shows delivered energy increases of 5 to 25 percent compared to constant current discharges of the same average current. The percentage-increase was a function of chopper frequency, the ratio of peak-to-average current, and the magnitude of the discharge current.

Because the chopper effects are of a complex nature, electric vehicle battery/speed controller interaction must be carefully considered in vehicle design to optimize battery performance.

INTRODUCTION

One widely used technique for motor speed control is the chopper (pulse) control (ref. 1). The motor speed is varied by increasing or decreasing the average current supplied to the motor. Electric vehicle designers have comparatively little data available on battery response to pulse discharges associated with these choppers in contrast with the more traditional alternative of direct current (d.c.) discharge.

The available energy and capacity of a battery are dependent on many factors, the most significant being the magnitude of the discharge current, with higher currents resulting in less delivered capacity. Tests completed on lead-acid batteries (ref. 2) demonstrated that when high levels of power are needed, pulse discharging can yield greater capacity and energy when compared to equivalent direct constant current discharging. However, when low levels of power are needed, the constant current method yields greater capacity and energy than the equivalent pulse current method. This crossover occurs when the discharge rates are greater than the "C" rate.

In view of the current efforts to develop efficient cost effective battery systems for electric vehicles, it is of great practical interest to quantify the effects on capacity associated with pulse discharging techniques when applied to NiZn cells. As part of the Department of Energy's program in electric vehicles, experiments were therefore undertaken to determine delivered battery capacity, energy, and power at various ratios of peak-to-average current. The parameters investigated were peak currents of 100, 200, 300, and 400 amperes and average values of 50, 100, 200, and 300 amperes at frequencies of 50, 100, and 500 Hz. Table I summarizes the test matrix used.

EXPERIMENTAL CELLS

The experimental cells used for the tests were manufactured by Yardney Electric Corporation for NASA under contract NAS3-20964. Two groups of four cells with consecutive serial numbers were chosen at random from a lot of 75 cells. The cells were designed so that when four are placed face to face they fit into a space having the dimensions of 10-3/8 in. long x 7-3/16 in. wide x 11-7/32 in. high (top of terminal). The Zn electrode separators used were NASA K-19. The negative (Zn) electrodes were pressed powder type construction and the positive (Ni) electrodes were of the electrochemically impregnated sintered type. The potassium hydroxide (KOH) electrolyte used was 34 percent by weight. The cells have a nominal capacity of 250 ampere-hours.

The formation of all cells consisted of three charge and discharge cycles after an initial "reverse charge" of the electroformed Ni electrode to an end cell voltage of -0.8 volt. This reverse charge was done to remove the residual charge in the Ni electrode, thus both the Ni and Zn electrodes are at the same level of charge. The cells were charged at constant current to 250 ampere-hours and discharged at 50 amperes to 1.0 volt with an actual capacity of about 210 ampere-hours.

EXPERIMENT PROCEDURE

The cells were tested as a 6.0-volt battery of four cells closely representing a mono-block 132 ampere-hour lead-acid battery in size, weight, and voltage. Each cell was

instrumented with an iron-constantan thermocouple located in the electrolyte near the top of the plates. The cells were tightly bound together with an additional thermocouple sandwiched between the faces of the middle cells near the center of the face.

The test equipment used to pulse discharge the cells was a chopper simulator shown in block diagram form in figure 1. A Darlington configured power transistor driven at appropriate variable pulse width and frequency (pulses per second) acted as the switching device. The power transistor was mounted on a water-cooled heat sink to dissipate the discharge energy. A non-inductive shunt was used to maintain the current signal in phase with the voltage signal as required to obtain accurate power measurements.

The battery voltage and current pulses were monitored on a calibrated dual-beam oscilloscope and photographed as required. In addition, a calobrated digital time and frequency domain waveform analyzer was used to calculate the delivered energy per pulse obtained by multiplying and integrating the instantaneous values of voltage and current with an accuracy of better than ± 0.5 percent. Capacity and energy was measured with a digital integrating ampere-hour meter to an accuracy of ± 1 percent. The average current (I) (shunt millivolt signal) and voltage (V) were read with an integrating digital volt meter capable of averaging the signals accurately over the range of test frequencies involved with ± 0.1 percent. The voltage and current waveforms were in phase at all frequencies thus assuring proper energy measurement.

Figure 2 represents an oscilloscope waveform of a chopper pulse of 400 amperes peak current, 25 percent duty cycle at 100 Hz. The average battery voltage was 6.50 volts.

The following equations represent the measured quantities:

$$c = \int_{t_s}^{t_f} i \, dt \qquad (1)$$

$$e = \int_{t_{on}}^{t_{off}} iv \, dt \qquad (2)$$

$$E = \int_{t_s}^{t_f} p \, dt \qquad (3)$$

$$\bar{p} = \frac{\int_{t_s}^{t_f} p \, dt}{t_f - t_s} \qquad (4)$$

where

t_s time at start of test
t_f time at end of test
t_{on} time at start of pulse
t_{off} time at end of pulse
i instantaneous current, amp
v instantaneous voltage, V
e energy per pulse
c capacity, A-hr
p power, W
$\bar{p}$ average power, W
E energy, W-hr

Equation (4) was calculated by dividing equation (3) by the quantity $(t_f - t_s)$.

The discharge tests were concluded at a battery terminal voltage of 4.0 volts. The cut-off for the pulse tests wa the average of the load and noload (off-time) voltages, and the load voltage for the constant current case. For a baseline comparison, a direct-current discharge equal in magnitude to the average current level was performed before and after each group of 50, 100, 200, and 300 ampere tests. Ambient and cell temperatures were recorded prior, during, and after each discharge. A 50 ampere constant current discharge was performed to remove the remaining cell capacity after all test conditions of 100 amperes or greater average currents.

The cells were recharged to 225 ampere-hours after every discharge at the C/8 rate (28A) after cell temperatures stabilized within 5° F of ambient.

RESULTS

Figure 3 is a plot of the capacity checks performed at the 50 ampere rate. The curves clearly indicate a loss in capacity. The original group I cells were removed from testing after 30 cycles when several cells in the pack were experiencing reversal near the end of a discharge. A new set of cells, group II, were formed to complete the test matrix at the 200 and 300 ampere level.

Figure 3 also shows an effect of average current rate on rate of capacity loss. A precipitous increase in capacity degradation is noted at the 300 ampere average current level.

The degradation of cell capacity with cycling makes the results biased according to the sequence in which the cells were run. In an attempt to eliminate the biased results, a linearized amount of capacity, determined from the slope of the curves in figure 3, was "added" to each successive cycle. In this manner, the capacity and energy results were normalized to the baseline results of the last formation cycle.

The biased raw data and normalized data, tabulated in tables II, III, IV, and V, summarize the numerical results of tests conducted at the various parameters and compares them to the constant current discharge at the same average current. In the case of 50 amperes average current, normalized pulsed conditions yielded equal or greater energy outputs of 10 to 15 percent at 500 Hz for all levels, than constant current. The trends of the data are an increase in energy with increasing frequency and a decrease in energy with an increase in the current pulse magnitude. The results of 100 amperes average

current, also show an increase in energy output with increasing frequencies with a maximum of 22 percent at 500 Hz, 300 and 400 amperes peak. However, the relationship of energy output to pulse magnitude is not straight-forward. Also all pulse tests at 50 Hz delivered energy below that of the direct current discharge energy. The 200 ampere average current data does not indicate any first-order relationships between energy output and frequency or pulse magnitude. The greatest energy output is seen at 500 Hz and 400 amperes pulse magnitude which is a 5 percent increase over the comparable direct current test. The results of tests of the 300 ampere average current at 400 amperes peak, show the energy delivered from the cells to increase with increasing frequency. A 9 percent energy output increase is noted at 500 Hz compared to the comparable direct current test.

Generally, pulse discharging NiZn cells at the lower current levels of 50 and 100 amperes yielded greater increases than at the higher discharge rates. These results are the inverse of the findings with lead-acid batteries where significant increase in energy and capacity were noted at the higher discharge rates (ref. 2).

The relationship between temperature and peak/average current is shown in figure 4. The rate of temperature rise, as expected, increased as the peak/average ratio increased. These thermal effects are consistent with the losses associated with higher peak currents. The quantitative effects of temperature on NiZn cell discharge capacity is not known. The higher generated temperatures associated with pulsing as compared to direct currents could contribute in part to the increased energy outputs obtained using pulse discharging.

Figure 5, average current versus capacity, shows the groupings of the pulsed and nonpulsed data. Except for a few cases, pulse discharging yielded more capacity. A plot of power versus energy is shown in figure 6. This curve also shows a greater energy output by pulsing at lower discharge rates.

CONCLUSION

The effects on delivered energy and capacity resulting from pulse discharge techniques on NiZn cells are complex. Pulse discharging generally yielded greater energy and capacity than the comparable constant current nonpulsed discharge test. These increases in energy amounted to 15, 22, 9, and 5 percent at 50, 100, 200, and 300 amperes average current, respectively. The greater increases were seen at discharges of low power levels that is, 50 and 100 amperes. This indicates that extended electric vehicle range could be achieved using pulse discharging (chopper) with a NiZn battery.

Temperature effects on NiZn battery performance are not known to the extent of making quantified corrections to the data. Higher temperatures were observed with increasing peak currents which could have contributed, in part, to the increases in energy and capacity associated with pulse discharging.

REFERENCES

1. Morrison, John L.: Electronic Control of Battery Electric Vehicles. Radio Electron. Eng., Vol. 42, Feb. 1972, pp. 91-100.

2. Cataldo, Robert L.: Response of Lead-Acid Batteries to Chopper - Controlled Discharge. NASA TM-73834 (Revised), DOE CONS/1044-1, Aug. 20, 1978, pp. 1-9.

TABLE I. - TEST MATRIX

Peak current				Average current	Frequency
400	300	200	100	50	50
			100	50	100
			100	50	500
				100	50
				100	100
				100	500
				200	50
				200	100
				200	500
				300	50
				300	100
				300	500

TABLE II. - TEST RESULTS AT 50 AMPERES AVERAGE CURRENT

Peak current, amp	Frequency, Hz	Mean power, W	Energy, W-hr		Capacity, amp-hr		Temperature rise, °C	Order of tests
			Raw	Normal	Raw	Normal		
50	D.C.*	300	1236	1236	206	206	12	1
400	50	293	1250	1265	213	216	22	2
300	50	297	1241	1275	209	215	21	3
200	50	300	1139	1192	190	199	18	4
100	50	307	1122	1194	183	194	15.5	5
400	100	312	1128	1261	188	202	23	6
300	100	309	1155	1292	192	209	21	7
200	100	317	1162	1327	191	211	14.4	8
100	100	317	1143	1317	185	208	13	9
400	500	335	1111	1323	172	198	23	10
300	500	331	1169	1400	183	212	20	11
200	500	328	1154	1399	182	213	17	12
100	500	330	1122	1407	179	213	13	13
50	D.C.*	294	1058	1205	168	206	13	14

*D.C. (direct current).

TABLE III. - TEST RESULTS AT 100 AMPERES AVERAGE CURRENT

Peak current, amp	Frequency, Hz	Mean power, W	Energy, W-hr		Capacity, amp-hr		Temperature rise, °C	Order of tests
			Raw	Normal	Raw	Normal		
100	D.C.*	596	834	887	147	149	19	1
400	50	590	845	884	146	150	23	2
300	50	610	751	822	129	135	17	10
200	50	614	780	852	131	139	15	8
400	100	601	902	989	155	165	24	3
300	100	617	784	892	133	145	18	9
200	100	618	828	936	138	152	15	7
400	500	645	954	1080	152	167	27	4
300	500	653	914	1074	147	164	22	5
200	500	632	809	956	132	151	16	6
100	D.C.*	631	726	878	118	139	22	11

*D.C. (direct current).

TABLE IV. - TEST RESULTS AT 200 AMPERES AVERAGE CURRENT

Peak current, amp	Frequency, Hz	Mean power, W	Energy, W-hr		Capacity, amp-hr		Temperature rise, °C	Order of tests
			Raw	Normal	Raw	Normal		
200	D.C.*	1182	1146	1184	198	200	25	1
400	50	1134	1123	1178	203	208	35	2
300	50	1164	1129	1199	199	206	31	3
400	100	1146	1112	1192	194	208	35	6
300	100	1155	1074	1181	188	205	30	7
400	500	1197	1158	1247	199	208	36	4
300	500	1142	1111	1163	192	204	31	5
200	D.C.*	1170	1076	1192	185	204	23	8

*D.C. (direct current.)

TABLE V. - TESTS RESULTS AT 300 AMPERES AVERAGE CURRENT

Peak current, amp	Frequency, Hz	Mean power, W	Energy, W-hr		Capacity, amp-hr		Temperature rise, °C	Order of tests
			Raw	Normal	Raw	Normal		
300	D.C.*	1747	786	854	140	147	25	1
400	50	1667	737	893	134	160.7	27	4
400	100	1708	810	907	146	159	28	2
400	500	1766	795	930	138	158	29	3
300	D.C.*	1712	656	858	117	151	21	5

*D.C. (direct current).

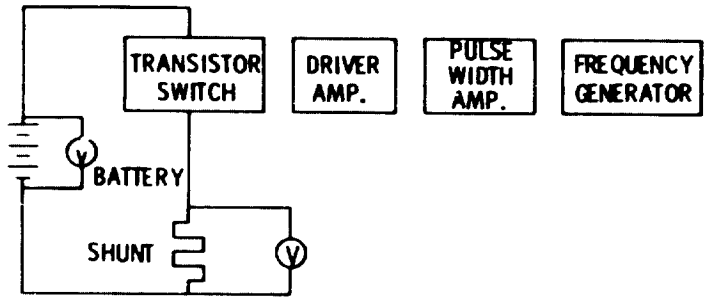

Figure 1. - Block diagram of chopper simulator

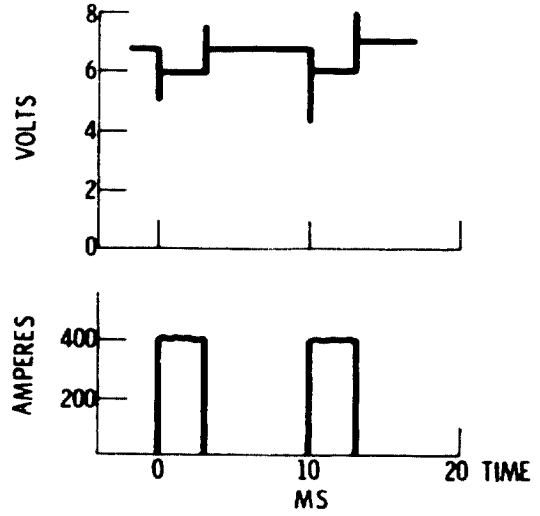

Figure 2. - Typical oscilloscope trace of the chopper simulator discharging a nickel zinc battery at 400 A peak current and 100 ampere average current at 100 Hz.

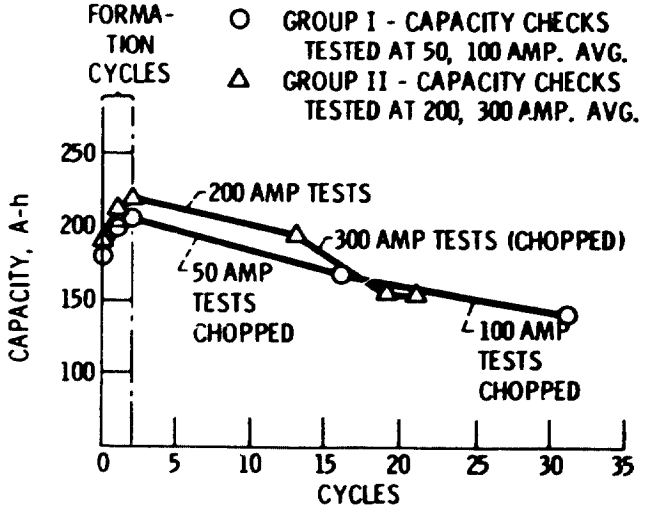

Figure 3. - 50 ampere capacity checks versus cycle number.

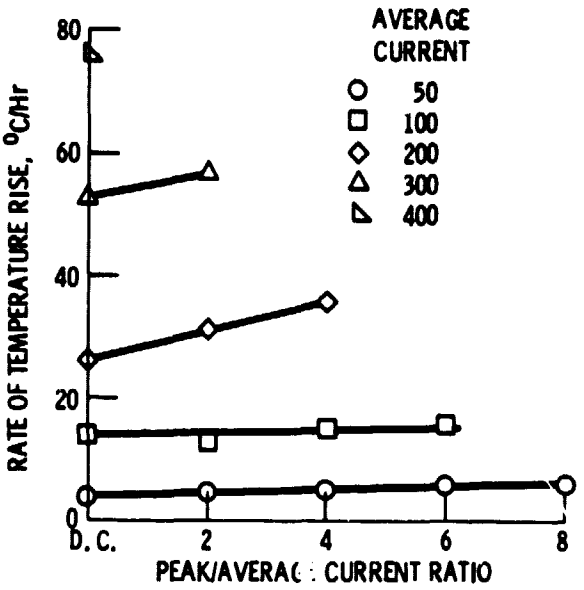

Figure 4. - Rate of temperature rise versus peak/average current ratio.

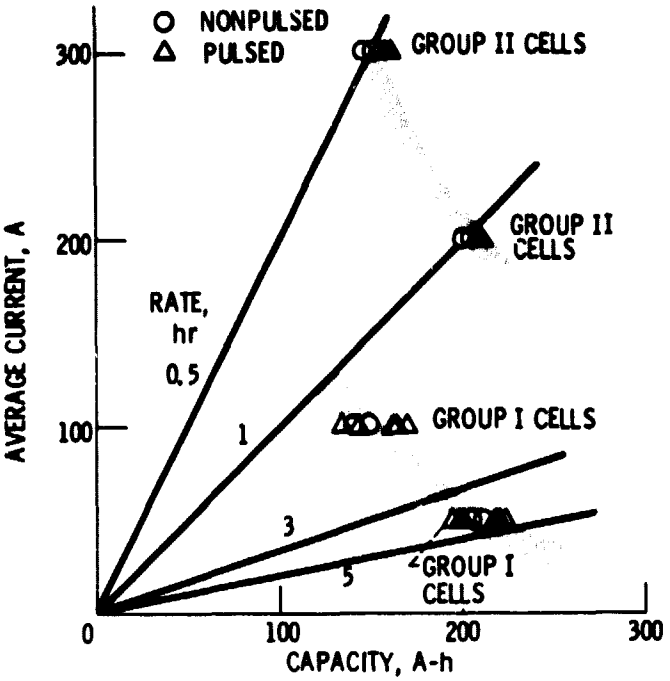

Figure 5. - Time average discharge current versus discharge capacity.

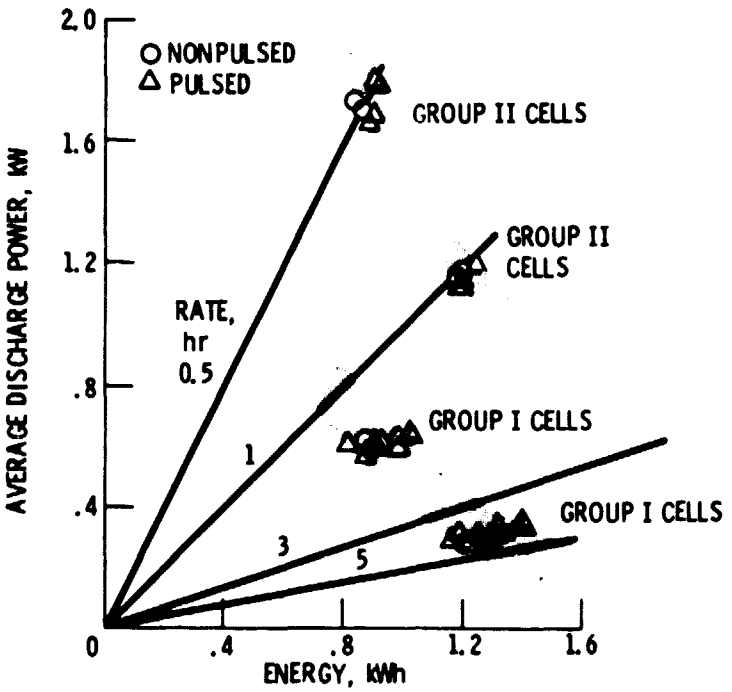

Figure 6. - Time average power versus energy.